

# Early ontogenic origin of the hematopoietic stem cell lineage

Yosuke Tanaka<sup>a</sup>, Misato Hayashi<sup>a</sup>, Yasushi Kubota<sup>a,1</sup>, Hiroki Nagai<sup>b</sup>, Guojun Sheng<sup>b</sup>, Shin-Ichi Nishikawa<sup>a</sup>, and Igor M. Samokhvalov<sup>a,2</sup>

<sup>a</sup>Laboratory for Stem Cell Biology, and <sup>b</sup>Laboratory for Early Embryogenesis, Center for Developmental Biology, RIKEN Kobe Institute, Kobe, Hyogo 650-0047, Japan

Edited by Mervin C. Yoder, Indiana University School of Medicine, Indianapolis, IN, and accepted by the Editorial Board January 30, 2012 (received for review September 26, 2011)

Several lines of evidence suggest that the adult hematopoietic system has multiple developmental origins, but the ontogenic relationship between nascent hematopoietic populations under this scheme is poorly understood. In an alternative theory, the earliest definitive blood precursors arise from a single anatomical location, which constitutes the cellular source for subsequent hematopoietic populations. To deconvolute hematopoietic ontogeny, we designed an embryo-rescue system in which the key hematopoietic factor *Runx1* is reactivated in *Runx1*-null conceptuses at specific developmental stages. Using complementary *in vivo* and *ex vivo* approaches, we provide evidence that definitive hematopoiesis and adult-type hematopoietic stem cells originate predominantly in the nascent extraembryonic mesoderm. Our data also suggest that other anatomical sites that have been proposed to be sources of the definitive hematopoietic hierarchy are unlikely to play a substantial role in *de novo* blood generation.

The developmental origin of hematopoiesis is obscured by the extreme mobility of blood cells. Probing the hematopoietic potential of cells from different anatomic locations in mammalian conceptuses has led to conflicting views on blood origin (1). It is generally thought that the first adult-type hematopoietic stem cell (HSCs) emerge *de novo* in the aorta-gonad-mesonephros (AGM) region of the midgestation embryo (2). Other vascular regions of the conceptus, such as the umbilical and vitelline arteries and the vascular labyrinth region of placenta, also harbor the earliest HSCs (3, 4), although their role in the generation of these stem cells is less clear (1). In addition to its well-known role in the establishment of “primitive” hematopoiesis, the visceral yolk sac is believed to serve as an independent source of some “definitive” hematopoietic progenitors (5, 6) but not adult-type HSCs. Cell-transplantation studies (7, 8) and our recent cell-tracing experiments have shown, however, that yolk sac precursor cells contribute to adult hematopoiesis (9). These data support the pioneering insight by Moore and Metcalf that the yolk sac is a primary source of definitive hematopoietic development (10). Nevertheless, it remains unclear whether the definitive hematopoiesis emerges from a single anatomical location in a discrete ontogenic event or from multiple ontogenic sources during an extended developmental period. To address this question, we devised an embryo-rescue system in which the key hematopoietic factor *Runx1* is reactivated in *Runx1*-null conceptuses in a controlled and stage-specific manner. We provide functional evidence that specification of the HSC lineage takes place early in ontogenesis, immediately after the start of gastrulation. Our results suggest that the nascent extraembryonic mesoderm is the major source of the HSC precursors.

## Results

***Runx1*<sup>+</sup> Vascular Endothelial (VE)-Cadherin<sup>+</sup> Yolk Sac Cells Display Lymphopoietic Potential.** To reexamine the origin of definitive hematopoiesis, we first tested whether the early yolk sac has a lymphopoietic potential. In contrast to previous observations (11), embryonic day (E) 7.5 yolk sac cells efficiently differentiated in the OP9 coculture system (Fig. S1C) into CD19<sup>+</sup>CD11b<sup>+</sup>

B cells with rearranged IgH loci (Table S1 and Fig. S1E and F). We characterized the phenotype of yolk sac cells producing B cells based on *Runx1* and VE-cadherin expression. More than 90% of VE-cadherin<sup>+</sup> yolk sac cells at the neural-plate stage are *Runx1*<sup>+</sup>, and a substantial fraction of the head-fold VE-cadherin<sup>+</sup> cell population still expresses *Runx1* (Fig. S1A and B). Only the double-positive *Runx1*<sup>+</sup>VE-cadherin<sup>+</sup> cells formed hematopoietic progenitor colonies on OP9 stroma (Fig. S1D) and differentiated into B cells (Fig. S1E). Thus, *Runx1*<sup>+</sup> yolk sac precursors express VE-cadherin and demonstrate lymphopoietic potential, although it is not clear whether the detected potential reflects the actual hematopoietic commitment *in vivo* or arises spontaneously *in vitro*.

**Rescue Tracing System Design.** To dissect the origin of definitive hematopoiesis in a noninvasive *in vivo* cell-tracing setup, we designed an embryo-rescue system in which *Runx1* is reactivated at specific stages of development. *Runx1* is strictly required for definitive hematopoietic development in a cell-autonomous fashion (12). Lethal vascular lesions in *Runx1*-null embryos have been reported to be secondary to the absence of definitive hematopoietic progenitors and HSCs (13). Recent conditional gene-knockout experiments have confirmed the early and critical role of *Runx1* in the process of mesoderm specification toward definitive blood-cell lineages (14). Early cell-autonomous function of *Runx1* can therefore serve as a marker of *de novo* hematopoiesis. If spatiotemporally restricted reactivation of *Runx1* expression in *Runx1*-null conceptuses occurs in competent precursor cells, it would lead to the rescue of definitive hematopoiesis and allow us to pinpoint its developmental origin (Fig. 1).

**Generation of a *Runx1*-MER-Cre-MER Null Allele.** Our rescue cell-tracing system employs a reactivatable “target” *Runx1*<sup>LacZ</sup> null allele and a “driver” null allele with the *MER-Cre-MER* gene fusion under control of the *Runx1* locus. The Cre-mediated excision of a transcription stop cassette (*STOP*) in the *Runx1*<sup>LacZ</sup> allele converts it into the fully functional *Runx1*<sup>Re</sup> allele (15). In conceptuses bearing these two alleles, gene reactivation is confined to cells expressing *Runx1* at the developmental stage at which tamoxifen is applied. One candidate for the driver allele, *Runx1*<sup>Cre</sup>

Author contributions: I.M.S. designed research; Y.T., M.H., Y.K., H.N., G.S., and I.M.S. performed research; G.S. and S.-I.N. contributed new reagents/analytic tools; Y.T., S.-I.N., and I.M.S. analyzed data; and I.M.S. wrote the paper.

The authors declare no conflict of interest.

This article is a PNAS Direct Submission. M.C.Y. is a guest editor invited by the Editorial Board.

Freely available online through the PNAS open access option.

<sup>1</sup>Present address: Division of Hematology, Respiratory Medicine and Oncology, Department of Internal Medicine, Faculty of Medicine, Saga University, Saga 849-8501, Japan.

<sup>2</sup>To whom correspondence should be addressed. E-mail: igors@cdb.riken.jp.

This article contains supporting information online at [www.pnas.org/lookup/suppl/doi:10.1073/pnas.1115828109/-DCSupplemental](http://www.pnas.org/lookup/suppl/doi:10.1073/pnas.1115828109/-DCSupplemental).

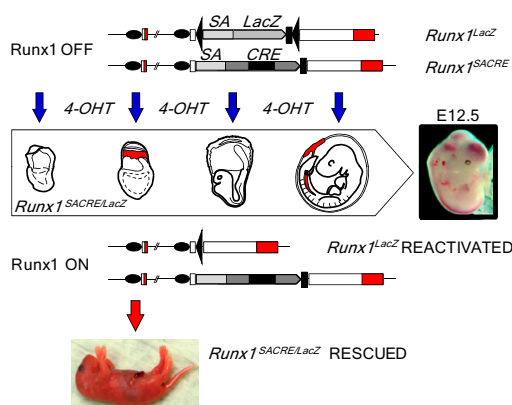


**Fig. 1.** Experimental strategy for deconvolution of the hematopoietic system development. The development of Runx1-null embryos can be rescued by maternal injection of 4-OHT at distinct stages of gestation. Upstream *Runx1* exons are represented by open boxes with coding regions in red. Black ovals, two promoters of the gene; black triangles, *loxP* sites; black rectangles, *STOP* cassettes; SA, splice acceptor sequence.

(9), was found to be hypomorphic and therefore not suitable for the embryo-rescue analysis. The *Runx1*<sup>Cre/Cre</sup> homozygotes successfully developed to term, but the newborn pups were unable to feed and died during the first day after birth. Analysis of *Runx1* transcription in the homozygotes revealed attenuation of gene expression initiated from the proximal promoter (P2),

whereas distal promoter (P1)-dependent expression was normal (Fig. S2 A–D).

To render the *Runx1*<sup>Cre</sup> allele nonfunctional, we introduced the mouse *Engrailed-2* splice acceptor (*En2SA*) sequence in front of the coding region (Fig. 2 E–G) in the same manner as for generation of the *Runx1*<sup>LacZ</sup> allele (15). In the new *Runx1*<sup>SACRE</sup> allele, the *En2SA* insertion places the *MER-Cre-MER* recombinase under the control of both *Runx1* promoters. All *Runx1*<sup>SACRE/SACRE</sup> and *Runx1*<sup>SACRE/LacZ</sup> embryos die around E12.5, exhibiting severe hemorrhagic phenotype and liver anemia characteristic for Runx1-null mutants (Fig. S2 H and I). Using *Rosa26R-LacZ* reporter mice, we have verified the *MER-Cre-MER* expression pattern in the day 8 conceptuses. Short-term 4-hydroxytamoxifen (4-OHT) exposure induced LacZ staining coinciding with the characteristic expression of *Runx1* at this stage of development (Fig. S3A). Similar analysis of the E9.5-activated embryos (Fig. S3B) confirmed the expression of the *MER-Cre-MER* recombinase in Runx1<sup>+</sup> embryonic territories (16).

**Efficient Recombination Across Tested Developmental Stages.** To evaluate the efficiency of ligand-dependent recombination driven by the *Runx1*<sup>SACRE</sup> allele, we measured the relative levels of adult hematopoietic cell labeling induced at early phases of blood development. To this end, we crossed *Runx1*<sup>SACRE/wt</sup> mice with the *Rosa26*<sup>R26R-eYFP/R26R-eYFP</sup> reporter mice (17) and injected pregnant dams with single 4-OHT doses at E7.5–E10.5. The recombination efficiency at each stage was measured as percentage of enhanced YFP<sup>+</sup> (eYFP<sup>+</sup>) cells in adult peripheral blood leukocytes (Fig. S3C). Injections at E7.5 with low doses of the ligand

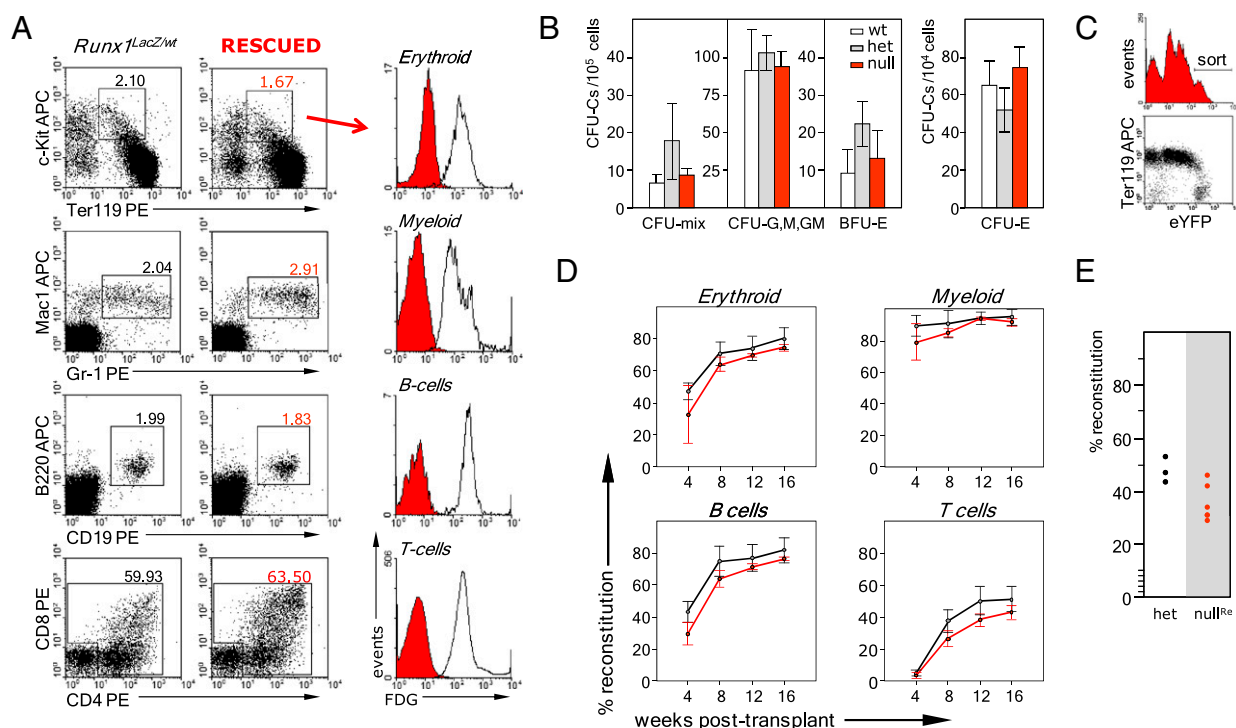


**Fig. 2.** Complete hematopoietic recovery in the E7.5-rescued Runx1-null embryos. (A) Major hematopoietic cell lineages in the rescued E16.5 Runx1-null embryos are LacZ<sup>+</sup>. Fetal liver cells and thymocytes from four embryos of each genotype from two litters were pooled for the analysis. Red histograms, cell fluorescence of the rescued hematopoietic cells; open histograms, cell fluorescence of the control *Runx1*<sup>LacZ/wt</sup> cells. Numbers here and elsewhere in FACS data indicate the percentage of respective cell populations. (B) Restoration of clonogenic hematopoietic progenitors in fetal livers of E16.5-rescued embryos. Data are mean  $\pm$  SD,  $n = 4$ . (C) Cell sorting of the rescued embryos for the long-term reconstitution assay. E16.5 fetal liver cells of six rescued and six control embryos from four litters were pooled, and donor eYFP<sup>high</sup> cells were sorted as shown in the histogram. Nearly all eYFP<sup>low</sup> cells belong to the erythroid lineage (FACS dot plot). (D) Competitive long-term reconstitution assay of the E7.5-rescued E16.5 fetal liver HSCs. Major hematopoietic lineages were defined as in Fig. S5. All recipients were reconstituted. Red lines, mean reconstitution levels by rescued donor cells (five recipients); black lines, mean reconstitution levels by control donor cells (four recipients). (Error bars: SD.) (E) Secondary transplantation of eYFP<sup>+</sup>Lin<sup>-low</sup> bone marrow cells isolated from the primary recipients.

(1–2 mg per dam) resulted in insignificant labeling of adult leukocytes ( $4.0\% \pm 3.7\%$ ,  $n = 6$ ). Increasing the dose to 5–6 mg dramatically enhanced the labeling of definitive hematopoietic precursors. The mean adult multilineage (Fig. S3D) contribution of cells labeled at E7.5 grew to the levels ( $34\% \pm 7.8\%$ ,  $n = 11$ ) substantially exceeding those reported earlier for the *Runx1<sup>Cre</sup>* allele activated by the same dose of 4-OHT (9). Under this regimen, the average recombination efficiency at E8.5 ( $67.9\% \pm 6.9\%$ ,  $n = 16$ ) was two times higher, and at E9.5 it was slightly higher ( $39.4\% \pm 5.4\%$ ,  $n = 5$ ) than at E7.5. There was a marked drop in recombination efficiency after the high-dose injections at E10.5, although the average level was still substantial ( $10.9\% \pm 4.4\%$ ,  $n = 9$ ), up to 18% in some cases. In summary, the recombination-efficiency analysis provided prerequisite information for comparing the embryo-rescue potential of 4-OHT injections made at different stages of gestation.

**Runx1-Null Embryos Can Be Rescued only at E6.5–E7.5.** To determine the stages at which *Runx1* reactivation can rescue the development of *Runx1*-deficient embryos, we crossed *Runx1<sup>LacZ/wt</sup>* to *Runx1<sup>SACRE/wt</sup>* mice and examined the outcome of single-dose maternal injections of 4-OHT delivered before initiation of definitive hematopoiesis in the fetal liver at E11.5. As shown in Table 1, high-dose ligand injections at nominal stages E6.5 and E7.5 rescued the *Runx1*-null phenotype (Fig. S3E) in 90–100% of ligand-exposed *Runx1<sup>SACRE/LacZ</sup>* conceptuses. The Mendelian frequency of genotyped *Runx1*-null embryos points to a low probability of unaccounted embryonic fatalities. Strikingly, low doses of the drug injected at E7.5, a regimen of a few percent recombination efficiency (Fig. S3C), also led to very robust embryo rescue (80–100%) tested at E16.5 or in the newborns.

All later reactivations at E8.0, E8.5, E9.5, and E10.5 (designated hereafter as “post-E7.5”) failed to rescue *Runx1*-null embryos from developing intense hemorrhaging and profound fetal liver anemia (Table 1 and Fig. S3F). This finding delineates a temporal window for the rescue-efficient gene reactivations so that, starting from E8.0, any residual ligand activity of the E7.5-injected drug cannot induce the corresponding *Runx1<sup>+</sup>* territories to contribute to the embryo rescue.

Pregastrulation injections at E5.5 were also ineffective, demonstrating the limited (less than 24 h) postinjection period of productive recombination in vivo, as evidenced by the fact that the E5.5-injected ligand did not restore *Runx1*-null embryo development despite the onset of rescue competence at E6.5. Of note, for the post-E7.5 stages, we used only the high 4-OHT dose regimen that, even at E10.5, produces significantly higher recombination efficiency compared with the rescue-positive low-

dose injections at E7.5 (Fig. S3C). It is therefore reasonable to assume that the failure of post-E7.5 injections reflects severe deficiency of the rescuing precursor cells in the entire conceptus at E8.0 and thereafter, rather than inefficiency of post-E7.5 gene reactivations.

Our results suggest that the critical ontogenetic function of *Runx1* is required specifically in E6.5–E7.5 precursor cells. At the neural-plate stage (E7.5), *Runx1* is expressed in extraembryonic mesoderm of the proximal yolk sac and chorion, as revealed by  $\beta$ -galactosidase reporter gene staining (16). The chorionic expression of *Runx1* at the late neural-plate stage was detected by in situ hybridization with a radioactive probe corresponding to the upstream coding region (18). Our in situ hybridization analysis with the downstream *Runx1* probe (Fig. S4) showed that *Runx1<sup>+</sup>* territory is restricted to the proximal yolk sac mesoderm in the neural-plate conceptuses. Because the rescue window includes the earlier stages (Table 1), in which either no *Runx1* is expressed in chorion (18) or the chorion has yet to be formed (Fig. S4), we concluded that the extraembryonic mesoderm settling in the proximal yolk sac region is the most likely source of rescued blood progenitors.

**Restoration of Definitive Hematopoiesis upon *Runx1* Reactivation at E7.5.** Next, we investigated hematopoiesis in E7.5-reactivated (treated in utero around E7.5 by the high dose of 4-OHT) *Runx1<sup>SACRE/LacZ</sup>* fetuses. FACS profiles of the rescued in vivo blood-cell populations at E16.5 were similar to the profiles of the control heterozygous cells (Fig. 2A), demonstrating the complete recovery of definitive hematopoiesis. Because Cre recombination removes the *LacZ* cassette from the *Runx1<sup>LacZ</sup>* allele (Fig. 1), the cells with the reactivated gene become labeled as *LacZ<sup>-</sup>*, allowing us to trace the progeny of rescued hematopoietic precursors because all E16.5 fetal blood cells, except enucleated erythrocytes, express *Runx1/LacZ* before recombination (Fig. 2A). All cells of major hematopoietic lineages in the E7.5-reactivated E16.5 *Runx1<sup>SACRE/LacZ</sup>* fetuses were *LacZ<sup>-</sup>* (Fig. 2A), indicating that all definitive hematopoietic lineages descend from the E7.5 de novo hematopoietic precursors that sustained reactivation of *Runx1*. The progeny of these precursor cells survive and develop independently of the *Runx1<sup>-</sup>* environment (Fig. S3E), which further emphasizes the cell-autonomous role of *Runx1* in hematopoietic ontogenesis.

Methylcellulose colony-formation assay of E16.5 fetal liver cells in the E7.5-reactivated embryos showed full restoration of definitive hematopoietic progenitors (Fig. 2B). For the HSC analysis, we crossed *Runx1<sup>LacZ/wt</sup>;<sup>Rosa26<sup>R26R-eYFP/R26R-eYFP</sup></sup>* and *Runx1<sup>SACRE/wt</sup>;<sup>Rosa26<sup>w/wt</sup></sup>* mice and injected pregnant females at

**Table 1. *Runx1* reactivation at specific developmental stages between E5.5 and E10.5**

Injection → analysis	Total embryos	<i>Runx1<sup>w/wt</sup></i>	<i>Runx1<sup>SACRE/wt</sup></i> and <i>Runx1<sup>LacZ/wt</sup></i>	<i>Runx1<sup>SACRE/LacZ</sup></i>		
				Total	Absorbed/ hemorrhage	Rescued, %
E5.5 → E12.5	34	9	19	6	6	0
E6.5 → E12.5	21	6	9	6	0	100
E7.5 → E16.5	82	18	44	20	2*	90
E7.5 → E16.5 (1–2 mg)	124	21	73	30	6	80
E7.5 → DPP1 (2 mg)	35	9	15	11	0	100
E8.0 → E12.5	50	8	31	11	11	0
E8.5 → E12.5	76	17	39	20	20	0
E9.5 → E12.5	38	12	18	8	8	0
E9.5 → E16.5	18	3	12	3	3	0
E10.5 → E12.5	119	36	51	32	32	0

The single injections of 4-OHT were of high drug doses (5–6 mg per dam), unless otherwise indicated. DPP1, first day postpartum.

\*The two absorbed embryos were found in a litter that also contained dead wild types and heterozygotes.

E7.5 with the high dose of 4-OHT. We then sorted eYFP<sup>high</sup> fetal liver cells from *Runx1*<sup>SACRE/LacZ</sup>;*Rosa26*<sup>R26R-eYFP/wt</sup> (null) (Fig. 2C) and *Runx1*<sup>SACRE/wt</sup>;*Rosa26*<sup>R26R-eYFP/wt</sup> (het) embryos for i.v. injections into irradiated recipients. The long-term competitive repopulation assay of the E7.5-rescued HSCs from *Runx1*-null E14.5 and E16.5 fetal livers did not reveal a significant difference in the reconstitution levels compared with the het controls (Fig. S5 and Fig. 2D), indicating that rescued HSCs function successfully in the adult hematopoietic environment for a prolonged period. Robust lymphoid development in adult environment underscores the full differentiation potential of HSCs descending from the E7.5 *Runx1*<sup>+</sup> territories. Moreover, secondary transplantation of the yolk sac-derived bone marrow cells from primary recipients, performed 12 mo after the primary transplantation, resulted in a successful long-term engraftment (Fig. 2E). These data demonstrate that the restoration of *Runx1* function at E7.5 leads to the full recovery of functional adult-type HSCs. In summary, the E7.5 *Runx1*<sup>+</sup> extraembryonic mesoderm is an ontogenic source sufficient for development of adult-type HSCs and entire definitive hematopoiesis.

*Runx1* is known to participate in the ontogenesis of motor and sensory neurons (19) as well as skeleton (20). The short period of active postinjection recombination and anatomically restricted expression of *Runx1* suggest that the E6.5–E7.5 gene reactivations are unlikely to rescue the development of non-blood-cell lineages. The blood-rescued *Runx1*-null pups were born apparently normal but were unable to feed and died within 1 d postpartum. Reactivation of the same *Runx1*<sup>LacZ</sup> allele in the *Tie2*<sup>+</sup> anatomic compartments led to similar postnatal mortality (21), which may result from abnormal skeletal or neural development (22, 23).

**Post-E7.5 Reactivations Fail to Recover Definitive Hematopoiesis.** We investigated the hematopoietic status of E11.5 *Runx1*-null embryos subjected to the post-E7.5 reactivations of *Runx1*. We did not see noticeable improvements in embryo survival (Fig. S3F) after 4-OHT injections at any of these stages. Only a high-density ( $5 \times 10^4$  cells per 35-mm dish) methylcellulose assay of fetal liver cells from the E8.5-reactivated embryos detected the presence of

a few hematopoietic progenitors, all with the recombined *Runx1* locus, whereas high-density cultures from E9.5- and E10.5-reactivated embryos were completely negative (Fig. S6A). Because of significantly reduced fetal liver cellularity in *Runx1*-null embryos, the colony forming cell (CFC) number per single fetal liver in E8.5-reactivated embryos was several hundred times lower than it was in the controls (Fig. S6B). The residual level of CFC restoration at E8.5 is probably too low for the rescue of the ontogenesis. Indeed, minimal recovery of at least a few percent of definitive hematopoietic progenitors (low drug doses at E7.5; Fig. S3C) appears to be necessary for efficient embryo rescue (Table 1). The absence of more differentiated erythroid CFCs (CFC-Es) after all post-E7.5 reactivations (Fig. S6C) indicates that these rare surviving progenitors are not functional in vivo. Thus, the post-E7.5 reactivations failed to rescue definitive hematopoietic progenitors, suggesting that either the corresponding hematopoietic sites do not contain mesodermal precursors of de novo hematopoiesis or the number of these precursors is below the limits of our assay system.

The AGM region is the only conceptus location that efficiently accumulates the hematopoietic progenitor and stem cell potential upon explant culture (2). We therefore investigated in detail the efficiency of 4-OHT-induced Cre recombination and the outcome of *Runx1* reactivation in the region. We first examined the labeling of E11.5 AGM region upon the Cre-recombinase activations at E8.5, E9.5, and E10.5. Efficient recombination is induced at all stages in the hemogenic endothelium of dorsal aorta (Fig. 3A). Next, we compared the CD45 expression profile of the AGM cells in E11.5 *Runx1*<sup>SACRE/LacZ</sup>;*Rosa26*<sup>R26R-eYFP/wt</sup> (null) and *Runx1*<sup>SACRE/wt</sup>;*Rosa26*<sup>R26R-eYFP/wt</sup> (het) embryos from the same litters exposed to high-dose 4-OHT for 24 h (Fig. 3B). In the het AGM, a significant fraction of the CD45<sup>+</sup> cell population was expressing eYFP after the E10.5 injections, whereas, in the null AGM, we did not detect CD45<sup>+</sup> definitive hematopoietic cells. Of note, in null and het embryos, very similar CD45<sup>-</sup> AGM cell populations became eYFP-labeled upon Cre-recombinase induction. In line with their embryo-rescue potential, E7.5 reactivations led to the appearance of intensely eYFP-labeled CD45<sup>+</sup> population in the E11.5 AGM region (Fig. 3D).

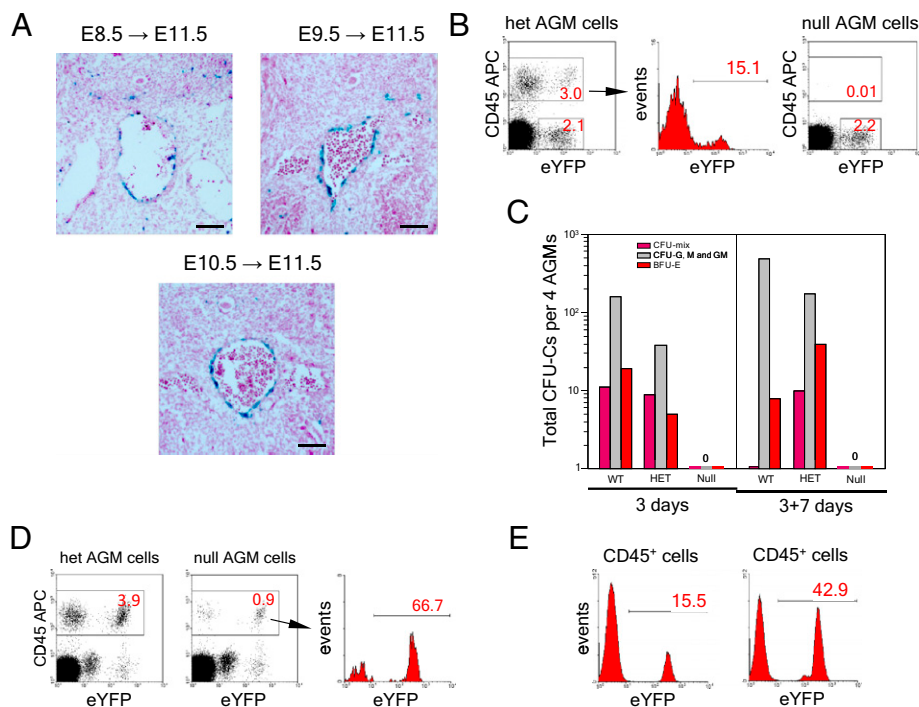


**Fig. 3.** E10.5 injections are unable to recover hematopoiesis in the *Runx1*-null AGM region. (A) Cell labeling in E11.5 AGM region after post-E7.5 inductions. (Scale bar: 200  $\mu$ m.) (B) Flow cytometry analysis of pooled AGM region cells (10 AGMs of three litters for each genotype) after the E10.5 induction. (C) Hematopoietic progenitor development in the two-step OP9 stroma culture of the pooled E11.5 AGMs (four AGMs for each genotype from two litters). The AGM regions were dissected 24 h after 4-OHT in utero induction. No exogenous cytokines were added to the culture medium. Zero denotes complete absence of hematopoietic colonies and cell clusters. (D) Emergence of CD45<sup>+</sup> cells in the AGM region (five AGMs of two litters for each genotype) after activation of Cre recombinase at E7.5. (E) Analysis of the eYFP labeling of *Runx1*<sup>SACRE/wt</sup> hematopoietic cells amplified in methylcellulose after the first step (Left) and the second step (Right) of the AGM explant culture on OP9 stroma.

Finally, using a two-step OP9 cell-culture system, we analyzed the hematopoietic potential of E11.5 AGMs from embryos exposed in utero to 4-OHT for 24 h. Generation of CFCs and the eYFP labeling of their CD45<sup>+</sup> progeny was measured after a 3-d AGM explant culture and after an additional 7-d progenitor expansion step (Fig. 3C). The eYFP cell labeling of hematopoietic progeny of het AGM regions increased typically by approximately threefold after the additional 7-d expansion step (Fig. 3E), suggesting that the E10.5 reactivation efficiently targets the AGM precursors of high proliferative potential. Complete absence of the hematopoietic progenitor recovery in the null AGM cultures (Fig. 3C) is therefore consistent with the notion that the post-E7.5 reactivations fail because of absence of competent hematopoietic precursors at these stages.

**In Vitro Reactivations Confirm the Early Onset of Definitive Hematopoiesis.** Although *Runx1* function in hematopoietic development is cell-autonomous, the *Runx1*-null microenvironment for de novo hematopoiesis may deteriorate nonspecifically during the abortive development, exerting a negative effect on post-E7.5 rescue attempts in vivo. To address this possibility, we performed a complementary series of *Runx1* reactivations in vitro using OP9 stroma as a model of normal embryonic microenvironment. In addition, culturing explanted embryo tissues (Fig. S7A) ensures an efficient 4-OHT penetration to the target *Runx1*-null cells.

In vitro gene reactivations in E7.5 *Runx1*<sup>SACRE/LacZ</sup> yolk sac explants markedly restored hematopoietic progenitors, demonstrating that our culture system supports the rescue of definitive hematopoiesis (Fig. S7B). In line with the results of the in vivo reactivations (Fig. S6), very few yolk sac progenitors were rescued at E8.5, but the later rescue attempts were completely unsuccessful (Fig. S7B). Culturing E7.5 and post-E7.5 *Runx1*-null embryo explants or embryonic cells in the presence of 4-OHT did not rescue the development of hematopoietic progenitors to any measurable extent (Fig. S7C–H). These data support the extraembryonic origin of primary hematopoietic precursors. We detected 4-OHT-dependent recombination of the *Runx1*<sup>LacZ</sup> target allele in VE-cadherin<sup>+</sup> cell fractions of nonhematopoietic *Runx1*-null post-E7.5 cultures, confirming the gene reactivation event (Fig. S7I). Notably, even nine pooled E10.5 caudal halves exposed to 4-OHT showed no recovery of any hematopoietic activity (Fig. S7H) despite very high in vitro recombination efficiency at this stage (Fig. S7I).

In summary, the in vitro experiments confirmed the results of our in vivo studies and suggested that the failed post-E7.5 rescue attempts in vivo were not attributable to a damaged microenvironment in *Runx1*-null conceptuses or inefficient penetration of the injected drug to target tissues. The outcome of our in vitro studies differs from previously published reports that the retroviral *Runx1* reactivation rescues the definitive hematopoiesis in vitro (24). However, it is difficult to exclude a possibility that *Runx1* has a strong reprogramming potential similar to its transcription network partners, PU.1 and C/EBP (25).

**Endothelialization of Hematopoietic Precursors.** To gain insight into the causes of the abrupt closing of the rescue window at around E8.0 (Table 1), we compared whole-mount LacZ stainings of E9.5–E11.0 *Runx1*<sup>LacZ/wt</sup> and *Runx1*<sup>LacZ/LacZ</sup> conceptuses. At this stage, the definitive progenitors can be identified among *Runx1*<sup>+</sup> blood cells within the developing yolk sac vasculature (Fig. 4). In E9.5 *Runx1*-null conceptuses, the majority of these blast-like cells are replaced by *Runx1*-expressing endothelium in the proximal part of yolk sac (Fig. 4 and Fig. S8A). These observations suggest that, upon *Runx1* inactivation, the yolk sac cells bearing characteristics of hemogenic endothelium fail to commit to the hematopoietic lineage and instead differentiate into endothelial cells. Consistently, *Runx1*-expressing cells disappear completely from the circulation by E10.5 in *Runx1*-null embryos (Fig. S8B). We

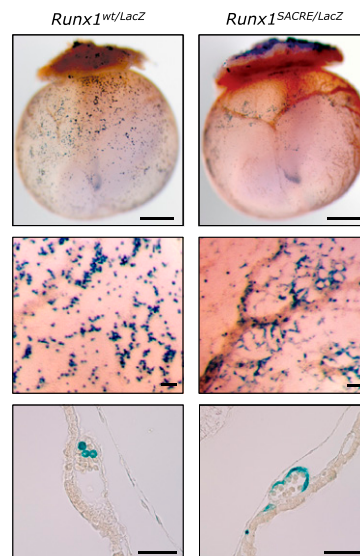


**Fig. 4.** Endothelialization of yolk sac hematopoietic cells in the absence of *Runx1*. (Top) Whole-mount LacZ staining of E9.5 conceptuses of two genotypes, *Runx1*<sup>wt/LacZ</sup> and *Runx1*<sup>SACRE/LacZ</sup>. In heterozygotes, single *Runx1*<sup>+</sup> definitive hematopoietic cells spread through the vasculature. In the absence of *Runx1*, cells with the active *Runx1* locus form a ring at the location retro-spectively corresponding to the E7.5 blood island primordia. (Scale bar: 500  $\mu$ m.) (Middle and Bottom) Higher magnification (Middle) and a dissected view (Bottom) of LacZ-stained E9.5 yolk sacs of the two genotypes. (Scale bar: 100  $\mu$ m.)

hypothesize that the endothelialization of de novo definitive hematopoietic precursors becomes irreversible at around E8.0 and leads to the failure of all rescue attempts thereafter.

## Discussion

We previously reported direct cell-lineage relationship between the yolk sac precursor cells and adult hematopoiesis (9). However, it was not determined whether *Runx1* expression in the early yolk sac is required for initiation of the HSCs development, and it remained formally possible that some uncommitted progeny of labeled yolk sac cells become incorporated into the midgestation hematopoietic sites and participate in the local specification of adult-type HSCs. In this paper, we provide functional evidence that the development of definitive hematopoietic progenitors and HSCs critically depends on *Runx1* expression in the nascent extraembryonic mesoderm. Using a unique in vivo *Runx1* reactivation system that closely recapitulates the process of de novo hematopoiesis, we identify the early extraembryonic mesoderm as a sufficient ontogenic source of HSC precursors that acquire the adult-type HSC phenotype later in gestation.

Despite uncovering the predominant role of early yolk sac in de novo hematopoiesis, our study leaves open the possibility that the yolk sac-derived definitive progenitors induce emergence of hematopoietic progenitors in the AGM region through paracrine interactions. However, the paracrine trigger would require clustering of the circulating progenitors on the dorsal aorta endothelium, suggesting the existence of a previously unknown non-cell-autonomous function of *Runx1* in hematopoietic development. Another possibility is that a few AGM-derived HSCs outcompete the stem cells originating from the yolk sac during development and/or postnatally, but our data on the high-level adult cell labeling induced at E7.5 (Fig. S3C) argue against this scenario. In any case, because early yolk sac operates as a primary and sufficient ontogenic source of the definitive hematopoiesis, the AGM region is essentially redundant for de novo blood generation and may represent a transitory niche for developing HSCs.

In our system, only one *Runx1* allele is reactivated in the rescued embryos. Although effects of the gene haploinsufficiency were reported for the midgestation dynamics of hematopoietic progenitors and HSCs, the earlier stages generally did not show any differences in this aspect (26). These observations render it unlikely that the early postgastrulation specification of the HSC lineage is influenced by the haploinsufficiency effects postulated for the progenitor distribution at E10.5–E12.5.

In this paper, we presented evidence for the existence of VE-cadherin<sup>+</sup> definitive hematopoietic precursors in the proximal yolk sac, which is consistent with a close ontogenic relationship between hemogenic endothelium and hemangioblasts or nascent lateral mesoderm (27). Finally, our findings must be compared with classical data on avian hematopoietic ontogenesis (28). It remains to be determined whether mammalian and avian de novo hematopoiesis differ significantly or whether a closer look at the presumed sites of blood-cell generation in chicken would reveal a more prominent role for the avian yolk sac (29).

## Materials and Methods

**Mice and 4-OHT Injections.** The *MER-Cre-MER* gene fusion (30) used in this work, as well as in a previous cell-tracing study (9), was a generous gift from Michael Reth (University of Freiburg, Freiburg, Germany). Targeted insertion of the cassette in the *Runx1* locus is described in Fig. S2. Other mouse strains used in the study, 4-OHT injection protocol, and staging of the injections were the same as in our previous publication (9). All animal experiments were carried out in accordance with the RIKEN guidelines for animal and recombinant DNA experiments.

**Cell Preparation and Flow Cytometry.** E7.5 yolk sacs, E9.5–E10.5 embryo caudal halves, and E11.5 AGM single-cell suspensions were prepared by brief treatment (1–2 min) of tissues with 0.05% trypsin/EDTA solution (Invitrogen) at 37 °C and pipetting into a single-cell suspension. Fetal livers and thymi were disrupted with 26-gauge needle in PBS containing 5% (vol/vol) FCS and

20 mM Hepes (pH 7.2). See *SI Materials and Methods* for description of flow cytometry analysis and the list of antibodies.

**Whole-Mount in Situ Hybridization, Immunostaining, and  $\beta$ -Galactosidase Assay.** See *SI Materials and Methods* for detailed description of the procedures.

**Reconstitution Experiments.** For in vivo cell transplantation, eYFP<sup>high</sup> fetal liver cells from E14.5 and E16.5 embryos were coinjected i.v. with bone marrow cells ( $2 \times 10^5$ , C57BL/6) into irradiated C57BL/6 mice. Repopulation was assayed in peripheral blood every 4 wk up to 16 wk posttransplantation. For secondary transplantations, eYFP<sup>+</sup>Lin<sup>low/-</sup> bone marrow cells from the primary recipient mice were used for injection of secondary recipients. Three months later, the YFP<sup>+</sup> cell engraftment was assessed in the peripheral blood by tail bleed. See *SI Materials and Methods* for detailed description of the experiments.

**Cell and Embryo Explant Culture.** Hematopoietic progenitor assay was performed in MethoCult GF M3434 medium (Stem Cell Technologies) according to manufacturer's recommendations. For the B-cell potential assay, explants and cells from individual mouse conceptuses were cultured on OP9 cell monolayers in the presence of 20 ng/mL murine Flt3 ligand (mFlt3-3L; R&D Systems), 20 ng/mL IL-7, and 10 ng/mL stem cell factor (SCF; PeproTech). For in vitro reactivation experiments, the concentration of 4-OHT was adjusted to 1  $\mu$ M. See *SI Materials and Methods* for a detailed description of the culture conditions.

**PCR Assay for *IgH* Rearrangement.** The analysis of *IgH* rearrangement in OP9 culture-derived CD19<sup>+</sup>CD11<sup>-</sup> cells was performed essentially as described in ref. 31. The details are given in *SI Materials and Methods*.

**ACKNOWLEDGMENTS.** We thank Shinichi Aizawa for providing us with T2 ES cells, Frank Costantini for *R26R-eYFP* mice, Hiroshi Kiyonari for generating the knock-in mouse strains, Doug Sipp for the text editing, and Marella de Bruijn for valuable suggestions. This work was supported by a grant from RIKEN Strategic Programs for Research and Development (President's Fund).

- Medvinsky A, Rybtsov S, Taoudi S (2011) Embryonic origin of the adult hematopoietic system: Advances and questions. *Development* 138:1017–1031.
- Medvinsky A, Dzierzak E (1996) Definitive hematopoiesis is autonomously initiated by the AGM region. *Cell* 86:897–906.
- de Bruijn MF, Speck NA, Peeters MC, Dzierzak E (2000) Definitive hematopoietic stem cells first develop within the major arterial regions of the mouse embryo. *EMBO J* 19:2465–2474.
- Ottersbach K, Dzierzak E (2005) The murine placenta contains hematopoietic stem cells within the vascular labyrinth region. *Dev Cell* 8:377–387.
- Palis J, Robertson S, Kennedy M, Wall C, Keller G (1999) Development of erythroid and myeloid progenitors in the yolk sac and embryo proper of the mouse. *Development* 126:5073–5084.
- Palis J, et al. (2001) Spatial and temporal emergence of high proliferative potential hematopoietic precursors during murine embryogenesis. *Proc Natl Acad Sci USA* 98:4528–4533.
- Weissman I, Papaioannou V, Gardner R (1978) Fetal hematopoietic origins of the adult hemolymphoid system. *Differentiation of Normal and Neoplastic Hematopoietic Cells*, eds Clarkson B, Marks PA, Till JE (Cold Spring Harbor Laboratory, New York), pp 33–47.
- Yoder MC, et al. (1997) Characterization of definitive lymphohematopoietic stem cells in the day 9 murine yolk sac. *Immunity* 7:335–344.
- Samokhvalov IM, Samokhvalova NI, Nishikawa S-I (2007) Cell tracing shows the contribution of the yolk sac to adult haematopoiesis. *Nature* 446:1056–1061.
- Moore MAS, Metcalf D (1970) Ontogeny of the haemopoietic system: Yolk sac origin of *in vivo* and *in vitro* colony forming cells in the developing mouse embryo. *Br J Haematol* 18:279–296.
- Cumano A, Dieterlen-Lievre F, Godin I (1996) Lymphoid potential, probed before circulation in mouse, is restricted to caudal intraembryonic splanchnopleura. *Cell* 86:907–916.
- Okuda T, van Deursen J, Hiebert SW, Grosveld G, Downing JR (1996) AML1, the target of multiple chromosomal translocations in human leukemia, is essential for normal fetal liver hematopoiesis. *Cell* 84:321–330.
- Takakura N, et al. (2000) A role for hematopoietic stem cells in promoting angiogenesis. *Cell* 102:199–209.
- Chen MJ, Yokomizo T, Zeigler BM, Dzierzak E, Speck NA (2009) Runx1 is required for the endothelial to haematopoietic cell transition but not thereafter. *Nature* 457:887–891.
- Samokhvalov IM, et al. (2006) Multifunctional reversible knockout/reporter system enabling fully functional reconstitution of the AML1/Runx1 locus and rescue of hematopoiesis. *Genesis* 44:115–121.
- Zeigler BM, et al. (2006) The allantois and chorion, when isolated before circulation or chorio-allantoic fusion, have hematopoietic potential. *Development* 133:4183–4192.
- Srinivas S, et al. (2001) Cre reporter strains produced by targeted insertion of *EYFP* and *ECFP* into the *ROSA26* locus. *BMC Dev Biol* 1:4.
- Lacaud G, et al. (2002) *Runx1* is essential for hematopoietic commitment at the hemangioblast stage of development *in vitro*. *Blood* 100:458–466.
- Theriault FM, Roy P, Stifani S (2004) AML1/Runx1 is important for the development of hindbrain cholinergic branchiovisceral motor neurons and selected cranial sensory neurons. *Proc Natl Acad Sci USA* 101:10343–10348.
- Lian JB, et al. (2003) Runx1/AML1 hematopoietic transcription factor contributes to skeletal development *in vivo*. *J Cell Physiol* 196:301–311.
- Liakhovitskaia A, et al. (2009) Restoration of Runx1 expression in the Tie2 cell compartment rescues definitive hematopoietic stem cells and extends life of Runx1 knockout animals until birth. *Stem Cells* 27:1616–1624.
- Liakhovitskaia A, et al. (2010) The essential requirement for Runx1 in the development of the sternum. *Dev Biol* 340:539–546.
- Stifani N, et al. (2008) Suppression of interneuron programs and maintenance of selected spinal motor neuron fates by the transcription factor AML1/Runx1. *Proc Natl Acad Sci USA* 105:6451–6456.
- Goyama S, et al. (2004) The transcriptionally active form of AML1 is required for hematopoietic rescue of the AML1-deficient embryonic para-aortic splanchnopleural (P-Sp) region. *Blood* 104:3558–3564.
- Feng R, et al. (2008) PU.1 and *C/EBP $\alpha$ / $\beta$*  convert fibroblasts into macrophage-like cells. *Proc Natl Acad Sci USA* 105:6057–6062.
- Cai Z, et al. (2000) Haploinsufficiency of AML1 affects the temporal and spatial generation of hematopoietic stem cells in the mouse embryo. *Immunity* 13:423–431.
- Lancrin C, et al. (2009) The haemangioblast generates haematopoietic cells through a haemogenic endothelium stage. *Nature* 457:892–895.
- Dieterlen-Lievre F (1975) On the origin of haemopoietic stem cells in the avian embryo: An experimental approach. *J Embryol Exp Morphol* 33:607–619.
- Nagai H, Sheng G (2008) Definitive erythropoiesis in chicken yolk sac. *Dev Dyn* 237:3332–3341.
- Zhang Y, et al. (1996) Inducible site-directed recombination in mouse embryonic stem cells. *Nucleic Acids Res* 24:543–548.
- Ehlich A, Martin V, Müller W, Rajewsky K (1994) Analysis of the B-cell progenitor compartment at the level of single cells. *Curr Biol* 4:573–583.